Effect of chromate ion on zinc electrowinning from acid sulphate electrolyte

J.-C. LIN,

Department of Mechanical Engineering, National Central University, Chung-Li, Taiwan 32054, ROC

S.-L. TSAI

Energy and Resources Laboratories, ITRI, Chu-Tung, Taiwan 31015, ROC

The effect of chromate ion and its interaction with antimony and glue on zinc electrowinning from acid sulphate electrolyte were studied. During electrolysis at $430\,A\,m^{-2}$ and $45\,°C$, the chromate ion was found to polarize the cathodic reaction resulting in a refined zinc deposit having a morphology featuring a vertical orientation of the zinc platelets. Although chromium did not codeposit, the current efficiency for zinc deposition was dramatically decreased in the presence of $> 1000\,mg\,dm^{-3}$. This effect became more pronounced when the electrolyte also contained additives such as antimony and glue.

1. Introduction

The presence of impurities in zinc electrolyte is a major concern for the electrolytic zinc industry. Over the past several years many investigations on the effects of impurities in zinc electrowinning have been published [1–7]. The hydrometallurgical processing of zinc alloys [8] can result in zinc electrolyte containing chromium as an impurity. Chromium is not encountered in zinc electrolyte produced from concentrates and it is not removed from the electrolyte by the usual purification methods [9]. Reagents such as glue and antimony are often added to purified zinc sulphate electrolyte to counteract the effect of trace impurities and to smooth the zinc deposit [10]. Thus, the present study was done to determine the effect on chromate ion, alone and in combination with glue and antimony, on the current efficiency of zinc deposition and on the zinc deposit morphology and orientation. Cyclic voltammetry was also employed to help elucidate the role of chromate ion in zinc electrowinning.

2. Experimental details

All the reagents used in this work were of E Merck analytical grade. The electrolytes were prepared by dissolving zinc sulphate ($ZnSO_4 \cdot 7H_2O$) and sulphuric acid in deionized water to produce a final concentration of $70\,g\,dm^{-3}$ Zn and $180\,g\,dm^{-3}$ H_2SO_4. Chromate ion, glue and antimony were added to the electrolyte as aliquots of dilute solutions of potassium chromate, gelatin, and potassium antimonyl tartrate, respectively, to give the required concentrations.

The electrowinning cell consisted of a 500 ml rectangular vessel of acrylic resin fitted with a cover with slots to hold the electrodes. A three-electrode assemblage consisting of a central cathode and two anodes was used. A saturated calomel electrode, fitted in a Haber–Luggin probe, functioned as the reference electrode. The cathodes which measured $80\,mm \times 30\,mm \times 1\,mm$, were fabricated from commercial purity aluminium sheet (99.6%). Either lead–silver alloy or high density graphite was used for the anodes, which measured $80\,mm \times 30\,mm \times 2\,mm$.

The aluminium cathodes were abraded with emery paper from 200 to 600 mesh, washed in an ultrasonic cleaner, rinsed with distilled water and acetone, then dried with hot air.

Electrowinning was conducted at $45\,°C$ for $2\,h$ at $430\,A\,m^{-2}$ current density. A potentiostat/galvanostat (HOKTO, HA-320) was employed as the power supply and for current control.

Sections of deposits were examined by X-ray diffraction (XRD) to determine their preferred orientation relative to the ASTM 4-0831 standard for zinc powder. These sections were also examined by scanning electron microscope (Jeol JSM 840) to determine their surface morphology. Selected deposits were also analysed for their chromium content by atomic absorption spectrophotometry (Perkin Elmer AAS 5000A).

The cyclic voltammetry experiments were conducted in a thermostatted three-electrode cell in an argon atmosphere. The working electrode was an aluminum sheet (99.6%) of surface area $100\,mm^2$ fixed with respect to a graphite counter electrode and a saturated calomel electrode (SCE) reference electrode. An electrochemical analyser (Model BAS 100B) was used to record the cyclic voltammograms. The working electrodes were prepared by wet

polishing on 600 grit emery paper, washed in an ultra-sonic cleaner, rinsed with distilled water and acetone, then dried with hot air. A voltammogram was obtained by varying the potential from -0.700 to -1.350 V vs SCE, then reverse scanned to the original starting potential. Various scanning rates were conducted; however, $2\,mV\,s^{-1}$ provided the most consistent results and was employed for this study.

3. Results and discussion

3.1. Effect of chromate ion on the deposit morphology and orientation

The effect of chromate ion on the morphology of 2 h zinc deposits electrowon at 45 °C and $430\,A\,m^{-2}$ from addition-free electrolyte containing $70\,g\,dm^{-3}$ Zn and $180\,g\,dm^{-3}$ H_2SO_4 is shown in Fig. 1(a) and 1(b). The deposit morphology consisted of hexagonal platelets, as indicated in Fig. 1(a). The platelets grow at low angles (0–30°) to the aluminium cathode and result in a basal orientation, similar to that reported previously [1, 2]. In comparison, a morphology consisting of platelets having a vertical orientation was obtained when $500\,mg\,dm^{-3}$ chromate ion was added to the electrolyte, Fig. 1(b). Obviously, chromate ion causes the crystallographic orientation of the deposit to change from basal to vertical. The crystallographic orientations for zinc deposits obtained for a variety of experimental conditions are summarised in Table 1. The various XRD peak intensities are presented as ratios to the ASTM standard values for zinc powder. Only planes having a peak intensity ratio greater than 0.50 are considered. Thus, the deposit orientation is preferred (0 0 2) (1 0 3) (1 0 1) (1 1 2) and (1 0 0), for chromate ion concentration of $100\,mg\,dm^{-3}$ (Table 1). Compared to the preferred orientation (0 0 2) for an addition-free electrolyte, this change is insignificant. However, increasing the chromate ion concentration to 300–$500\,mg\,dm^{-3}$ results in the deposits having a preferred vertical orientation, i.e. (1 0 2) (1 1 0) (1 0 3)

for $300\,mg\,dm^{-3}$, and (1 0 1) (1 1 0) (1 1 2) (1 0 3) for $500\,mg\,dm^{-3}$, respectively. Increasing the chromate ion concentration to $1000\,mg\,dm^{-3}$ changes the deposit orientation to preferred (0 0 2) and (1 0 1); i.e. a random-basal orientation.

The combined effect of chromate ion and antimony is shown in Fig. 2. Figure 2(a) shows a deposit with preferred basal orientation that was obtained in the presence of $0.04\,mg\,dm^{-3}$ antimony. The hexagonal zinc platelets are relatively larger and are oriented at lower angles than those shown in Fig. 1(a). Figure 2(b) shows a deposit having refined platelets with a random orientation that was electrowon in the presence of $0.04\,mg\,dm^{-3}$ Sb and $100\,mg\,dm^{-3}$ chromate ion. From Table 1, the deposit orientation for the addition of $0.04\,mg\,dm^{-3}$ Sb is preferred (0 0 2) (1 0 3) and (1 1 0); whereas the deposit orientation is preferred (0 0 2) (1 0 1) (1 0 3) (1 1 2) (1 0 2) and (1 1 0) in the presence of $0.04\,mg\,dm^{-3}$ Sb and $100\,mg\,dm^{-3}$ chromate ion. At $0.4\,mg\,dm^{-3}$ antimony, the deposit orientation is preferred (0 0 2) (1 0 3) (1 0 2) (1 0 1) and (1 1 0) but it changes to preferred (1 0 1) (1 0 0) (1 1 0) and (1 0 2) as $100\,mg\,dm^{-3}$ chromate ion is added. The effect of chromate ion evidently becomes significant in the presence of antimony at concentrations as low as $100\,mg\,dm^{-3}$. This phenomenon may possibly arise from an inter-action between antimony and chromate ion and is discussed later.

Organic additives, e.g. gums and animal glues affect the crystal growth of zinc deposits in a manner oppo-site to that of antimony; thus, the zinc platelets are reduced in size and grow vertically. The deposit depicted in Fig. 3(a), in which zinc hexagonal plate-lets grow at high angles (70–90°) to the aluminium substrate was obtained for an electrolyte containing $15\,mg\,dm^{-3}$ glue. When $100\,mg\,dm^{-3}$ chromate ion and $15\,mg\,dm^{-3}$ glue are both present in the electro-lyte, the deposit, illustrated in Fig. 3(b), appears to be both more compact and also of finer grain size than the deposit shown in Fig. 3(a). This deposit has

Table 1. Effect of chromate ion, antimony and glue on the orientation of 2 h zinc deposits electrowon at 430 A m^{-2} and 45 °C

Additives or impurity/ mg dm^{-3}	Orientation of zinc deposits (ratio to ASTM standard)*						
	(0 0 2)	(1 0 0)	(1 0 1)	(1 0 2)	(1 0 3)	(1 1 0)	(1 1 2)
Addition-free	1.89	0.05	0.08	0.03	0.16	0.10	0
100 chromate	1.89	0.60	0.62	0.38	0.96	0.05	0.57
300 chromate	0.11	0.08	0.46	3.45	1.64	1.81	0.39
500 chromate	0.43	0.45	1.00	0.38	0.60	0.71	0.61
1000 chromate	1.47	0.88	1.00	0.17	0.28	0.38	0.3
0.04 Sb	1.89	0.20	0.43	0.48	0.88	0.71	0.30
0.04 Sb + 100 chromate	1.06	0.40	1.00	0.59	0.84	0.52	0.70
Sb 0.4	1.89	0.23	0.62	0.83	1.08	0.52	0.48
Sb 0.4 + 100 chromate	0.47	0.83	1.00	0.62	0.32	0.76	0.48
15 glue	0.02	0.70	0.68	1.07	0.68	0.38	0.35
15 glue + 100 chromate	0.19	0.78	1.00	0.69	0.68	0.53	1.3
15 glue + 0.04 Sb	0.26	0.48	1.00	0.55	0.80	0.81	1.09
15 glue + 0.04 Sb + 100 chromate	0.28	0.43	1.00	0.41	0.48	0.57	0.39
15 glue + 0.4 Sb	0.66	0.43	1.00	0.45	0.80	0.67	0.39
15 glue + 0.4 Sb + chromate	0.75	0.45	1.00	0.62	0.76	0.62	0.48

* (0 0 2) 0.53; (1 0 0) 0.40; (1 0 1) 1.00; (1 0 2) 0.38; (1 0 3) 0.25; (1 1 0) 0.27; (1 1 2) 0.23.
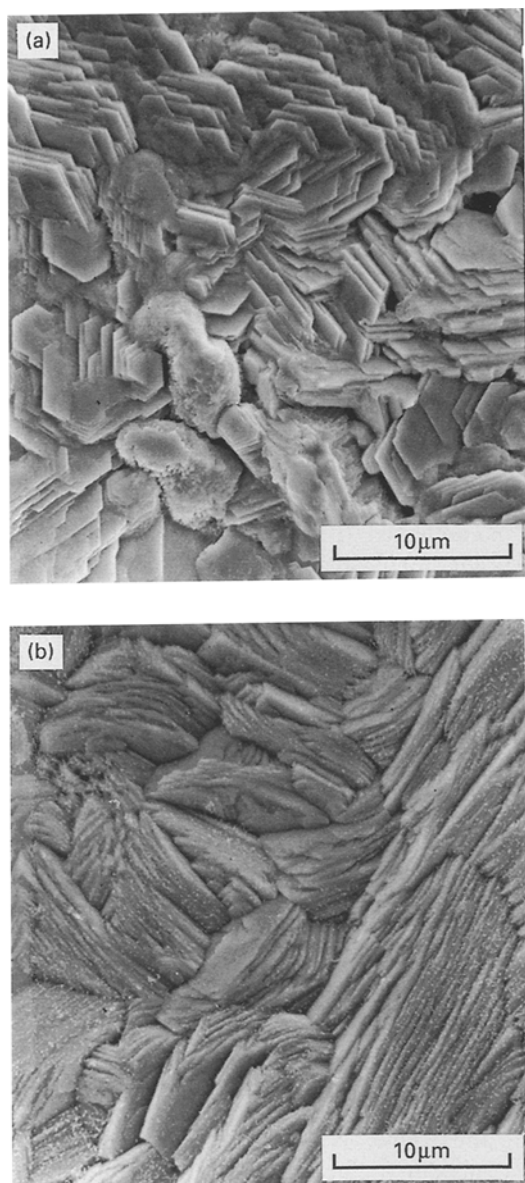
Fig. 1. SE micrographs showing the morphology of 2 h zinc deposits from (a) addition-free electrolyte and (b) electrolyte containing 500 mg dm^{-3} chromate ion.

Fig. 2. SE micrographs showing the morphology of 2 h zinc deposits from electrolyte containing (a) 0.04 mg dm^{-3} antimony and (b) 0.04 mg dm^{-3} antimony and 100 mg dm^{-3} chromate ion.

a smooth surface and its refined platelets are more vertically aligned. The data in Table 1 indicate a change in deposit orientation from (1 0 2) (1 0 0) (1 0 1) and (1 0 3), and for the addition of 15 mg dm^{-3} glue, to (1 1 2) (1 0 1) (1 0 0) (1 0 2) (1 0 3) and (1 1 0) the combination of 100 mg dm^{-3} chromate ion and 15 mg dm^{-3} glue.

In another case, an electrolyte containing 15 mg dm^{-3} glue and 0.04 mg dm^{-3} antimony gave a random oriented zinc deposit; i.e. (1 1 2) (1 0 1) (1 1 0) (1 0 3) and (1 0 2). When 100 mg dm^{-3} chromate ion was added to this electrolyte, the deposit platelets became more vertically aligned, e.g. predominantly preferred (1 0 1) (1 1 0) as indicated in Table 1.

The presence of chromate ion generally results in a change in the crystallographic orientation of the zinc deposit from basal to a vertical regardless of whether additives are present or not. In the absence of
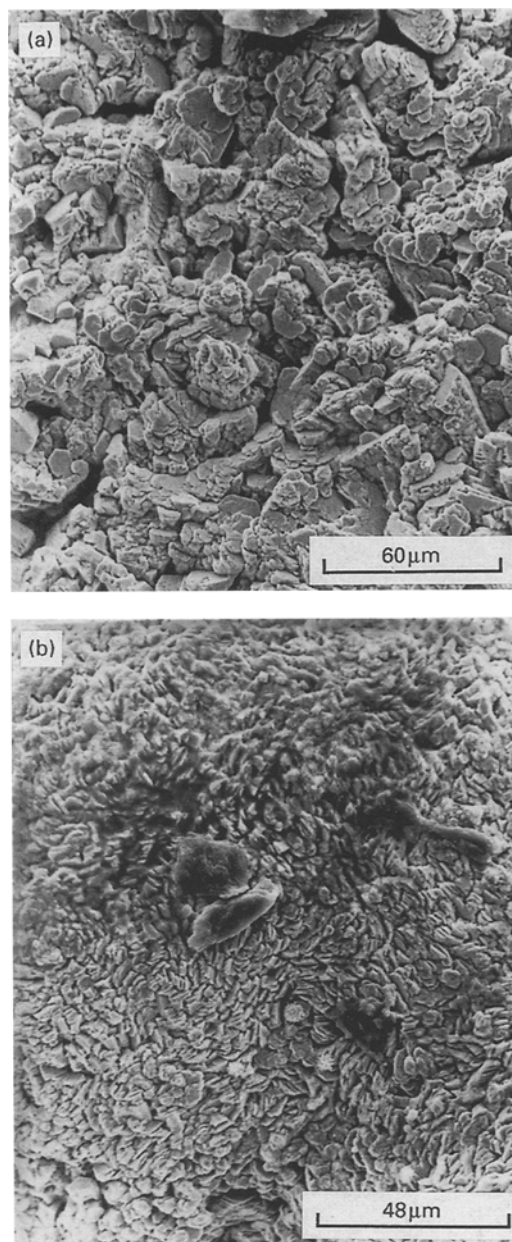
additives, the vertical orientation was not obvious until the chromate ion concentration reached 300 mg dm^{-3}. However, in the presence of glue and antimony a chromate ion concentration of 100 mg dm^{-3} was sufficient to change the deposit orientation to vertical.

Analysis of zinc deposits by X-ray diffractions and their aqua regia solutions by atomic absorption spectrophotometry revealed that chromium is not present in the zinc deposit, even if the concentration of chromate ion in electrolyte is high (up to 10 000 mg dm^{-3}). This suggests that chromate ion only plays a role in the polarization of zinc deposition.

3.2. Effect of chromate ion on cyclic voltammetry

The cyclic voltammograms for zinc deposition in the presence of antimony and chromate ion are compared to that for an addition-free electrolyte in
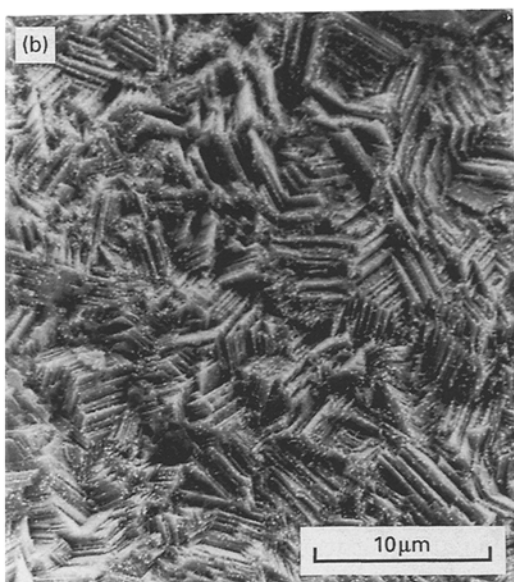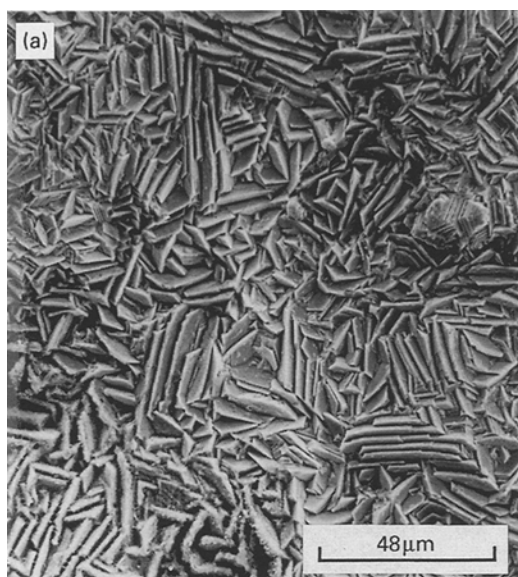
Fig. 3. SE micrographs showing the morphology of 2 h zinc deposits electrowon from electrolyte containing (a) $15 \, mg \, dm^{-3}$ glue and (b) $15 \, mg \, dm^{-3}$ glue and $100 \, mg \, dm^{-3}$ chromate ion.

Fig. 4. Cyclic voltammograms obtained for zinc deposition from addition-free electrolyte (curve (a), – – –), in the presence of $0.04 \, mg \, dm^{-3}$ antimony (curve (b), –·–·–), and in the presence of $500 \, mg \, dm^{-3}$ chromate ion (curve (c), ——).

Fig. 4. For a typical voltammogram, the cycle starting from $-0.70 \, V$ goes through a region of low current until the decomposition potential (ϕ_{dp}), where the cathodic current increases steeply and zinc deposition commences [11]. Beyond ϕ_{dp}, the cathodic current increases with decreasing potentials. At $-1.35 \, V$, the scan is reversed, which results in a current decrease that subsequently reaches zero at the cross-over potential (ϕ_{cop}); the current then becomes anodic corresponding to the dissolution of the deposited zinc [11]. An anodic peak is reached and zinc dissolution is complete on return to the starting point. The difference between the cross-over and decomposition potentials is a measure of the nucleation overpotential (NOP) for zinc deposition onto an aluminum substrate [12].

In Fig. 4, comparing curves (a) (addition-free) and (b) (addition of $0.4 \, mg \, dm^{-3}$ antimony), the cathodic portion of cyclic voltammogram curve (b) shifts to
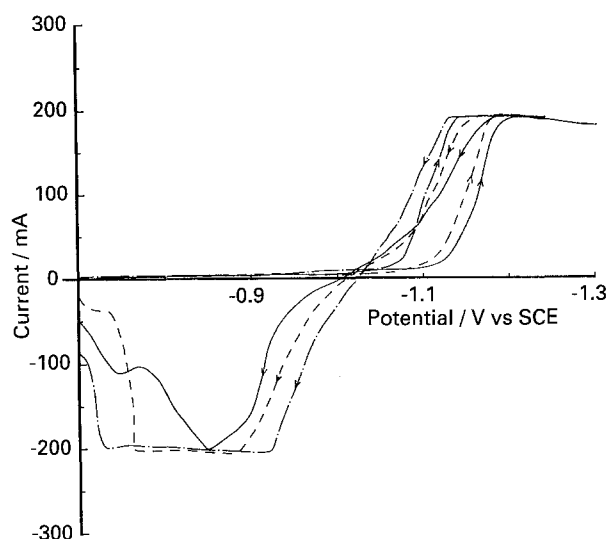
the left which consequently produces a less negative decomposition potential and indicates depolarization. On the contrary, curve (c) is shifted to the right of curve (a) owing to the addition of $500 \, mg \, dm^{-3}$ chromate ion, resulting in an increase in polarization. The polarization caused by $500 \, mg \, dm^{-3}$ chromate ion is, to an extent, similar to that observed for $15 \, mg \, dm^{-3}$ glue (not shown in Fig. 4 for clearness). Glue is obviously a stronger polarizer than chromate ion since the same polarization is exerted by a smaller concentration of the former. In the absence of other additives, increasing the chromate ion concentration from 50 to $1000 \, mg \, dm^{-3}$ shifts ϕ_{dp} to the right indicating an increase in polarization. At chromate ion concentrations $> 1000 \, mg \, dm^{-3}$, the electronegative shift of ϕ_{dp} is less; however, the cathodic current becomes greater prior to reaching ϕ_{dp}, Fig. 5. This current, which occurs prior to zinc

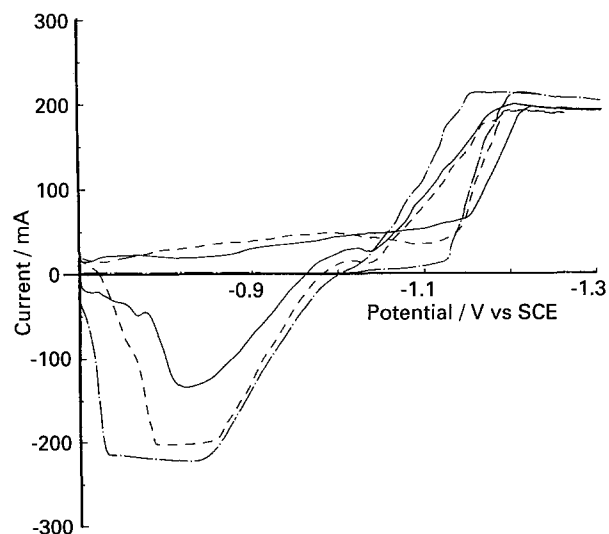Fig. 5. Cyclic voltammograms obtained for zinc deposition from electrolytes containing 1000 (curve (a), –·–·–), 5000 (curve (b), – – –), and $10\,000 \, mg \, dm^{-3}$ (curve (c) ——), chromate ion.
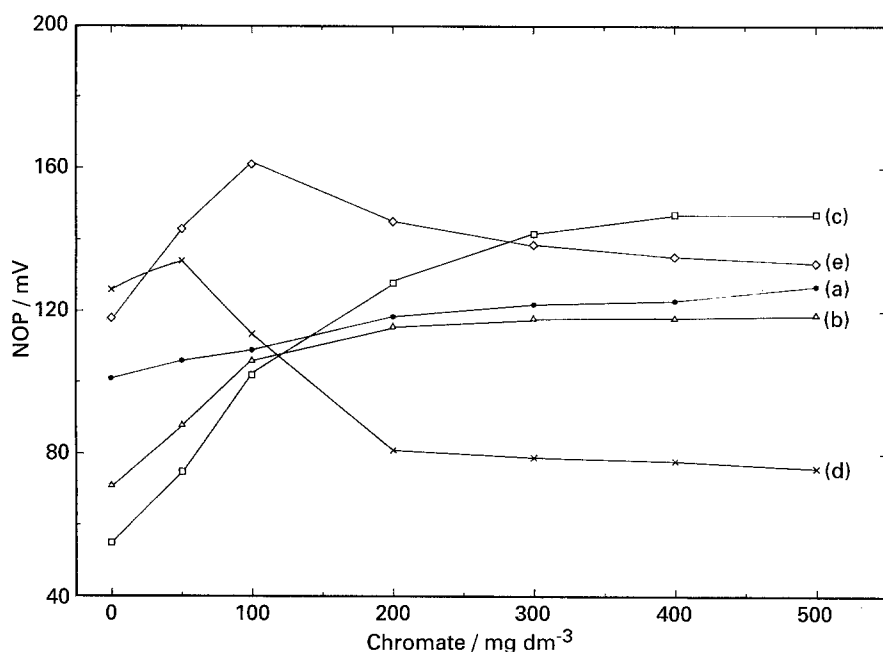
Fig. 6. Chromate ion effect on the nucleation overpotential (NOP) obtained for zinc deposition from various electrolytes. ($\bullet$, (a)) Addition-free; ($\triangle$, (b)) $0.04\,mg\,dm^{-3}$ Sb; ($\square$, (c)) $0.4\,mg\,dm^{-3}$ Sb; ($\times$, (d)) $15\,mg\,dm^{-3}$ glue; ($\diamond$, (e)) $0.04\,mg\,dm^{-3}$ Sb + $15\,mg\,dm^{-3}$ glue.

deposition, increases as the chromate ion concentration is increased from 1000 to $10\,000\,mg\,dm^{-3}$. It was observed that as the chromate ion concentration was increased, the hydrogen evolution became more vigorous and the current efficiency for zinc deposition decreased (81% for $1000\,mg\,dm^{-3}$, 38% for $5000\,mg\,dm^{-3}$ and 14% for $10\,000\,mg\,dm^{-3}$). According to Fig. 5, ϕ_{dp} shifts slightly to the right with increasing chromate ion concentration from 1000 to $10\,000\,mg\,dm^{-3}$, indicating an increase in zinc deposition polarization. On the reverse scan, Fig. 5, a current hump occurs after ϕ_{cop} $-1.020\,V$ for chromate ion concentrations of 5000 and $10\,000\,mg\,dm^{-3}$. The hump increases in height as the chromate ion concentration increases. In an electrolysis experiment conducted at the potential corresponding to this hump, the colour of the local solution around the cathode surface changed from orange to green, indicating that Cr(VI) is reduced to Cr(III).

A plot of NOP against chromate ion concentration is shown in Fig. 6 for various systems. Curves (a), (b) and (c) indicate that the NOP rapidly increases with increasing chromate ion concentration from $0-300\,mg\,dm^{-3}$, and then levels off between $300-500\,mg\,dm^{-3}$ chromate ion. Curves (d) and (e) show that the NOP initially increases to a maximum ($134\,mV$ for (d) and $162\,mV$ for (e), respectively) with increasing chromate ion concentration ($50\,mg\,dm^{-3}$ for (d) and $100\,mg\,dm^{-3}$ for (e)). This is subsequently followed by a drastic decrease at $300\,mg\,dm^{-3}$ and then levels off at $300-500\,mg\,dm^{-3}$ chromate ion. For curves (a), (b) and (c), the variation of NOP with chromate ion concentration depends on the concentration of antimony: in the absence of antimony, the NOP (curve (a)) slowly increases with increasing chromate ion concentration from $0-500\,mg\,dm^{-3}$; whereas in the presence of antimony ($0.04\,mg\,dm^{-3}$ Sb for curve (b) and $0.4\,mg\,dm^{-3}$ Sb for curve (c), respectively), the NOP increases much more rapidly from an initially lower value;

this is attributed to depolarization by antimony. At less than $100\,mg\,dm^{-3}$ chromate ion, the NOP for addition-free electrolyte is greater than that for $0.04\,mg\,dm^{-3}$ Sb which in turn is greater than that for $0.4\,mg\,dm^{-3}$ Sb. This suggests that the depolarization of antimony plays an important role for chromate ion concentration less than $100\,mg\,dm^{-3}$, and this depolarization is cancelled out by the polarization due to chromate ion concentration $> 100\,mg\,dm^{-3}$. At concentrations greater than $100\,mg\,dm^{-3}$, chromate ion is the dominant influence on zinc deposition polarization. The increase in NOP, curve (c), is greater than that for curve (b). This unexpectedly high NOP, which occurs as a consequence of $0.4\,mg\,dm^{-3}$ Sb and $> 200\,mg\,dm^{-3}$ chromate ion, is interesting and is discussed later.

Curve (d) indicates the effect of chromate ion on NOP in the presence of $15\,mg\,dm^{-3}$ glue. This NOP slowly increases from 126 to $134\,mV$ with chromate ion increasing from 0 to $50\,mg\,dm^{-3}$, then sharply decreases to $81\,mV$ ($200\,mg\,dm^{-3}$ chromate ion), and subsequently levels off. Curve (e) indicates the effect of chromate ion in the presence of $0.04\,mg\,dm^{-3}$ Sb and $15\,mg\,dm^{-3}$ glue. The NOP is initially $118\,mV$ in the absence of chromate ion, increasing rapidly to $161\,mV$ with increasing chromate ion ($100\,mg\,dm^{-3}$), and then decreases slowly to $138\,mV$ ($300\,mg\,dm^{-3}$ chromate ion) and subsequently levels off at $136\,mV$ for a higher concentration of chromate ion ($300-1000\,mg\,dm^{-3}$).

3.3. Dependence of current efficiency on chromate ion

The dependence of current efficiency on chromate ion concentration is indicated in Fig. 7. The data were obtained for a constant current density of $430\,A\,m^{-2}$ at $45\,°C$ for 2 h. Curve (a) displays the effect of chromate ion concentration on the current efficiency obtained for zinc electrowinning from an addition-free electrolyte. The current efficiency gradually
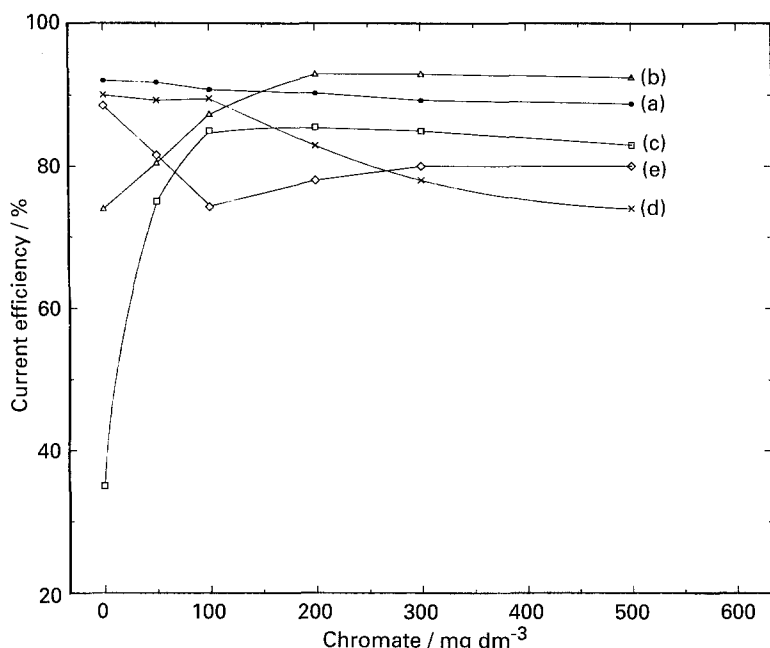
Fig. 7. Plots of current efficiency against chromate ion concentration obtained for zinc deposition at $430 \, A \, m^{-2}$ current density at $45 \, ^\circ C$ for $2 \, h$ from various electrolytes. ($\bullet$, (a)) Addition-free; ($\triangle$, (b)) $0.04 \, mg \, dm^{-3}$ Sb; ($\square$, (c)) $0.4 \, mg \, dm^{-3}$ Sb; ($\times$, (d)) $15 \, mg \, dm^{-3}$ glue; ($\diamond$, (e)) $0.04 \, mg \, dm^{-3}$ Sb $+ \, 15 \, mg \, dm^{-3}$ glue.

decreases from 92 to 88% with increasing chromate ion concentration from 0 to $500 \, mg \, dm^{-3}$. The current efficiency becomes less at chromate ion concentration $> 500 \, mg \, dm^{-3}$; e.g. 81% for 1000, 38% for 5000 and 14% for $10000 \, mg \, dm^{-3}$ chromate ion. The effect of chromate ion and its interaction with antimony is indicated in curves (b) and (c), Fig. 7. In the absence of chromate ion, antimony decreases current efficiency more severely at higher concentrations; e.g. 73% for 0.04 and 36% for $0.4 \, mg \, dm^{-3}$ Sb, respectively. The current efficiency markedly increases as a result of increasing concentration of chromate ion. Curve (b) demonstrates that an interaction between chromate ion and $0.04 \, mg \, dm^{-3}$ Sb enhances the current efficiency. The highest current efficiency, i.e. 94% was obtained for chromate ion concentration $\geqslant 200 \, mg \, dm^{-3}$. Curve (c) shows that the current efficiency increases more steeply from a lower value (36%) to 82% with the interaction between $0.4 \, mg \, dm^{-3}$ Sb and chromate ion (0–$100 \, mg \, dm^{-3}$). The current efficiency then levels off for chromate ion concentration greater than $100 \, mg \, dm^{-3}$. Curve (d) indicates the effect of $15 \, mg \, dm^{-3}$ glue and its interaction with chromate ion. The current efficiency ($\sim 90\%$), remains unchanged with increasing chromate ion concentration to $100 \, mg \, dm^{-3}$; then pronouncedly decreases to 75% as the chromate ion concentration is increased to $500 \, mg \, dm^{-3}$. Curve (e) shows the effect of $0.04 \, mg \, dm^{-3}$ Sb and $15 \, mg \, dm^{-3}$ glue alone and with chromate ion on current efficiency. In the absence of chromate ion the current efficiency is less than that obtained in both addition-free and glue-containing electrolytes. The current efficiency decreases to 75% with increasing chromate ion to $100 \, mg \, dm^{-3}$ but it increases to 80% with further increase in chromate ion concentration to $500 \, mg \, dm^{-3}$.

A plot of current efficiency against the corresponding NOP values is shown in Fig. 8. Although there is

some scatter in the data points, particularly those for $100 \, mg \, dm^{-3}$ chromate ion, the plot indicates that a maximum current efficiency occurs at NOP values of 100-120 mV. A similar CE–NOP correlation was observed for antimony–glue addition to Kidd Creek zinc electrolyte [13].

4. Reaction mechanism

The result obtained for effect of chromate ion on zinc electrowinning may be interpreted in terms of Epelboin's model for zinc deposition which includes H_{ads} and Zn^+_{ads} as adsorbed intermediates [14]. Hexavalant chromate (Cr VI) is the dominant species when
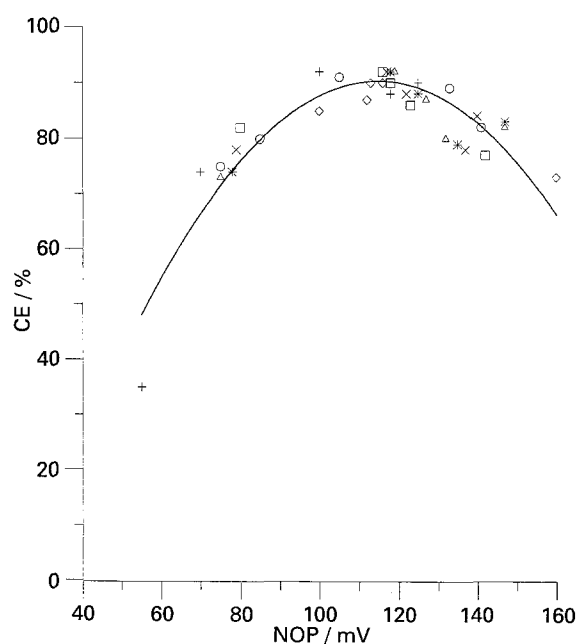

Fig. 8. Plot of current efficiency against nucleation overpotential obtained for electrolytes containing various concentration of chromate ion, antimony and glue. (+) 0, (o) 50, ($\diamond$) 100, ($\square$) 200, ($\times$) 300, (*) 400 and ($\triangle$) 500 chromate $mg \, dm^{-3}$.

chromate ion is dissolved in strong acid [15] and it plays an important role in cathode film formation during chromium electroplating [16]. In addition-free zinc electrolyte, the adsorption of Cr(vi) at the cathode could interfere with the formation of H_{ads} and Zn^+_{ads}, hence polarizing the zinc deposition reaction. Thus at chromate ion concentration $> 300\,mg\,dm^{-3}$, the NOP (polarization) increases, Fig. 6, the CE decreases, Fig. 7 and the zinc deposition morphology, consists of vertically oriented platelets, Fig. 1(b).

The failure to detect chromium in the zinc deposits can be explained by the fact that deposition of chromium metal from Cr^{6+} solutions is possible only within certain limits of the CrO_3/SO_4^{2-} ratio which ranges from 18.2 to 127.5 [17]. The impossibility of depositing chromium from strongly acidic solutions below pH 1.8 also has been demonstrated by other researchers [18–22]. The electrochemical reduction of Cr^{6+} was investigated by Lee and Sekine [22], who observed that only two reactions occurred, i.e. the reduction of Cr^{6+} to Cr^{3+} and hydrogen evolution.

The increase in cathodic current prior to zinc deposition observed on the forward scans of the cyclic voltammograms (Fig. 5) may be due to the adsorption of Cr(VI). This current increases with increasing chromate ion concentrations from 1000 to $5000\,mg\,dm^{-3}$. The hump that appears during the reverse scan (Fig. 5), is probably due to hydrogen evolution that results from the enhanced dissolution of the zinc deposition due to the reduction of Cr(vi) to Cr(iii). This is substantiated by a change in the colour of the electrolyte from orange to green in the vicinity of the cathode. The result is a marked decrease in CE and a very porous zinc deposit, consistent with zinc re-solution.

To explain the depolarizing effect of antimony, Fukubayashi [23] suggested a mechanism which involved the formation of hydrides in the double layer. In the presence of chromate ion the depolarization caused by the possible formation of hydrides may be hindered by the formation of a passive film due to Cr(vi) adsorption [16]. As a result, as shown in Fig. 6, the NOPs for 0.04 and $0.4\,mg\,dm^{-3}$ Sb have a similar value as that for addition-free for chromate ion at $100\,mg\,dm^{-3}$. At chromate ion concentration $> 200\,mg\,dm^{-3}$, the NOP with $0.4\,mg\,dm^{-3}$ Sb is greater than that with $0.04\,mg\,dm^{-3}$ Sb. This unusual result may be rationalized by the oxidative character of chromic acid with respect to the organic portion (tartrate) of the antimony complex. The hydroxy groups (–C–OH) in tartrate are oxidized by Cr(vi) to carbonyl group (–C=O) [24]. This product may absorb on the cathode (rather than cause a hydride formation) and result in synergism with chromate ion. The synergistic effect is more pronounced at higher concentrations of antimonyl tartrate. The combined effect of glue and chromate ion gives rise to either polarization or depolarization, depending on the concentration of chromate ion. At $< 100\,mg\,dm^{-3}$ chromate ion aids the adsorption of glue enhancing

polarization and results in a higher NOP, Fig. 6 (curve (d)). Subsequently, the NOP dramatically decreases with increasing chromate ion concentration. This is attributed to the interaction between glue and chromate ion. Chromate ion is a strong oxidant and its strength increases with increasing concentration. Glue in acidic solution is subject to degradation into amino acids [12, 23]. The degradation is believed to be strongly enhanced in the presence of a strong oxidant (chromic acid). The degraded products may adsorb in the double layer and function as a tartrate anion in forming hydrides; consequently, zinc deposition is depolarized. At $15\,mg\,dm^{-3}$, glue is completely degraded and the NOP levels off.

As glue and antimony are added together, the depolarization with antimony is balanced by the polarization with glue. Consequently, the NOP in Fig. 6 is between the values obtained for the single additions of these species. The effect of chromate ion in this case indicates that the simultaneous adsorption of glue and chromate ion dramatically increase the NOP. The depolarization caused by products of glue degradation then counteracts the polarization due to the products of antimonyl tartrate oxidation. Consequently, the NOP gradually decreases and levels off, as shown in Fig. 6 (curve (e)).

5. Conclusions

The effect of chromate ion and its interaction with glue and antimony on zinc electrowinning were determined. Chromate ion polarized zinc deposition resulting in a deposit morphology consisting of vertically oriented zinc platelets having a refined grain size. High concentrations of chromate ion; e.g. $> 1000\,mg\,dm^{-3}$, resulted in excessive hydrogen evolution together with re-solution of the zinc deposit, possibly due to reduction of adsorbed Cr (vi) to Cr (iii) at the cathode. Certain combinations of antimony and chromate ion maximized the current efficiency for zinc deposition, whereas the added presence of glue caused a decrease in current efficiency due to excessive polarization.

The results obtained in the study indicate that quality zinc deposits can be electrowon from electrolyte containing $\leqslant 1000\,mg\,dm^{-3}$ chromate ion. The addition of antimony improves the current efficiency and deposit quality. The presence of chromate ion provides sufficient polarization for zinc deposits so that the addition of glue to the electrolyte is not necessary. A correlation was observed to exist between the current efficiency and nucleation overpotential such that the CE is maximized when the NOP is between 100 and 120 mV.

Acknowledgements

References

[1]   R. C. Kerby and C. J. Krauss, 'Lead–Zinc–Tin '80' (edited by J. M. Cigan, T. S. Mackey and T. J. O'Keefe), TMS–AIME, New York (1979) p. 187.

[2]   M. K. Gupta, B. L. Gupta and R. Raghavan, *Hydrometall.* 22 (1989) 379.

[3]   I. Nirdosh, R. K. Kalia and S. V. Muthuswami, *ibid.* 20 (1988) 203.

[4]   J. F. Collins and A. M. Wolsky, A 'White Paper' prepared for the Waste Products Utilization Office of Industrial Programs US Department of Energy (1987).

[5]   D. J. Mackinnon, J. M. Brannen and P. L. Fenn, *J. Appl. Electrochem.* 17 (1987) 1129.

[6]   I. W. Wark, *ibid.* 9 (1979) 721.

[7]   D. R. Fosnacht and T. J. O'Keefe, *ibid.* 10 (1980) 495.

[8]   J.-C. Lin, Proceedings of ROC and ROK Bilateral Workshop on Mineral Beneficiation, Hydrometallurgy and Environmental Controls, Mining Research and Service Organization, Taiwan, ROC (1980) pp. 217–230.

[9]   S.-L. Tsai and J.-C. Lin, *Bull. CIMME: Mining & Metallurgy* 34(4) (1990) 116.

[10]   A. C. Scote, R. M. Pitblado, G. W. Barton and A. R. Ault, *J. Appl. Electrochem.* 18 (1988) 120.

[11]   B. A. Lamping and T. J. O'Keefe, *Met. Trans.*, 7B (1976) 551.

[12]   R. C. Kerby, H. E. Jackson, T. J. O'Keefe, and Yar-Ming Wang, *Met. Trans. B*, 8B (1977) 661.

[13]   D. J. Mackinnon, R. M. Morrison, J. E. Mouland and P. E. Warren, *J. Appl. Electrochem.* 20 (1990) 728.

[14]   I. Epelboin, M. Ksouri and R. Wiart, *J. Electrochem. Soc.* 122 (1975) 1206.

[15]   M. Pourbaix, 'Atlas of Electrochemical Equilibria', Pergamon Press, New York (1966) p. 261.

[16]   B. N. Popov, R. E. White, D. Slavkov and Z. Koneska, *J. Electrochem. Soc.* 139 (1992) 91.

[17]   G. Isserlis, in 'Industrial Electrochemical Processes' (edited by A. T. Kuhn) Elsevier, New York (1971) p. 355.

[18]   A. Radwan, A. El-Kiar, H. A. Farag, and G. H. Sedahmed, *J. Appl. Electrochem.* 22 (1992) 1161.

[19]   J. P. Hoare, A. H. Holden and M. A. LaBoda, *Plat. Surf. Finish* 67(3) (1980) 42.

[20]   J. P. Hoare, *J. Electrochem. Soc.* 130 (1983) 1475.

[21]   R. R. Lloyed, W. T. Rawles and R. G. Feeney, *Trans. Electrochem. Soc.* 89 (1946) 443.

[22]   J. S. Lee and T. Sekine, *Denki Kagaku* 44 (1976) 176.

[23]   H. H. Fukubayashi, T. J. O'Keefe and W. C. Clinton, US Bureau of Mines, Report of Investigations (1974) No. 7966.

[24]   F. A. Cotton and G. Wilkinson, 'Advanced Inorganic Chemistry', 4th edn., John Wiley & Sons, New York (1980) p. 471.